PAPER

Check for updates

Air oxidized activated carbon catalyst for aerobic oxidative aromatizations of N-heterocycles†

Lukas Enders,[a] David S. Casadio, [iD][a] Santeri Aikonen, [iD][a] Anna Lenarda, [iD][a] Tom Wirtanen, [iD][a] Tao Hu, [iD][b] Sami Hietala, [iD][a] Lucília S. Ribeiro, [iD][c] Manuel Fernando R. Pereira [iD][c] and Juho Helaja [iD]*[a]

A simple "reagent-free" thermal air treatment turns active carbon into a mildly oxidized material with increased quinoidic content that catalytically dehydrogenates saturated N-heterocycles to the corresponding aromatic compounds. Thermal decarboxylation improves the activity of the catalyst further, making it overall more efficient compared to other widely used carbocatalysts such as oxidized carbon nanotubes, graphene oxide and untreated active carbons. The substrate scope covers 1,2,3,4-tetrahydroquinolines (THQ), 1,2,3,4-tetrahydro-β-carbolines and related N-heterocyclic structures. The developed protocol also successfully dehydrogenates 3-(cyclohexenyl)indoles to 3-aryl indoles, opening a concise transition metal-free approach to (hetero)biaryls as exemplified with the synthesis of the core structure of progesterone receptor antagonist. Hammett plots, deuterium KIE measurements and computations at DFT level suggest that bimolecular hydride transfer mechanism is more likely to operate between THQs and the *o*-quinoidic sites of the catalyst, than the addition–elimination hemiaminal route. Comparison of structural parameters and catalytic performance of various oxidized carbon materials, prepared by different oxidative and optional post treatments, revealed that quinoidic content and surface area correlate with the obtained yields, while carboxylic acid content has a clear inhibiting effect for the studied oxidative dehydrogenations (ODHs). The carbocatalyst itself can be prepared from inexpensive and environmentally benign starting materials and its catalytic activity can be enhanced by a simple thermal oxidation in air that produces no reagent waste. Furthermore, oxygen is used as terminal oxidant, and the carbocatalyst is recyclable at least six times without a notable loss of activity.

Introduction

Activated carbons (ACs) are highly versatile materials with a wide range of applications from medicinal use to water purification and catalytic processes.[1] Among ACs' many interesting properties, high surface area and extensive porosity are the epicenter of their success in these fields. In catalysis, ACs have traditionally been used as supports for transition metal composites or nanoparticles but also, in growing numbers, as catalysts on their own merit.[2] As a

matter of fact, carbocatalysis has been known for almost over a century, but the growing demand for greener catalytic processes has fueled its further development in the last decades.[3–5]

From sustainable chemistry perspective, carbocatalysis is becoming an increasingly interesting concept: heterogeneous materials derived from abundant second row elements can promote reactions that are usually either performed with stoichiometric reagents or catalysed by transition metals. As a result, both reagent waste and demand for critical metals are reduced – both key aspects in green chemistry. Moreover, in oxidations, when (atmospheric) oxygen is employed to regenerate carbocatalyst's active sites, water and/or hydrogen peroxide is the only by-product generated.[6,7]

Alongside ACs,[3–12] other carbon allotropes such as carbon nanotubes (CNTs),[13–15] nanodiamonds (NDs), graphene oxides (GOs),[16–18] and nanohorns, have been employed as catalysts (Scheme 1) for organic transformations.[19,20] Gas-phase dehydrogenations of hydrocarbons in particular have been extensively studied with these materials, with received yields comparable to those of AC.[21] In gas-phase the oxidative
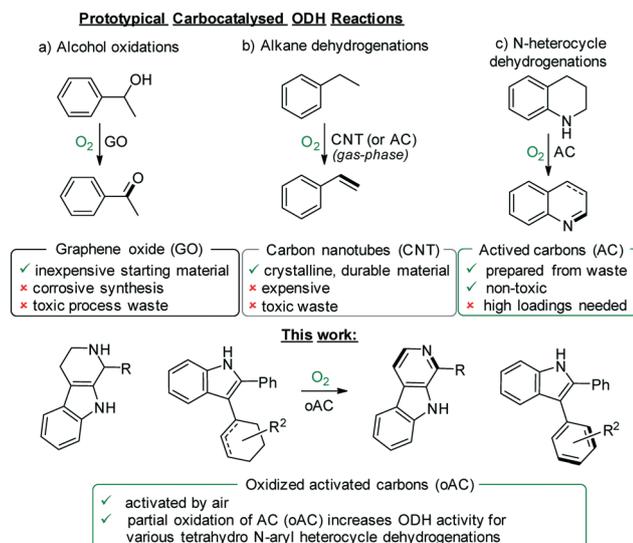
[a] *Department of Chemistry, University of Helsinki, A. I. Virtasen aukio 1, P.O. Box 55, 00014 Finland. E-mail: juho.helaja@helsinki.fi*
[b] *Research Unit of Sustainable Chemistry, Faculty of Technology, University of Oulu, 90014 Oulu, Finland*
[c] *Laboratory of Separation and Reaction Engineering-Laboratory of Catalysis and Materials (LSRE-LCM), Faculty of Engineering, University of Porto, 4200-465 Porto, Portugal*

† Electronic supplementary information (ESI) available: Materials; methods; synthetic procedures; and ICP-MS, NMR, XPS, TPD analyses, including copies of relevant spectra (PDF), computational details and XYZ parameters. See DOI: 10.1039/d1cy00878a

5962 | *Catal. Sci. Technol.*, 2021, **11**, 5962–5972

This journal is © The Royal Society of Chemistry 2021

Scheme 1 Frequently reported carbocatalytic ODH reactions of organic substrates by various carbon materials (above) (a) ref. 16–18, b) ref. in 8–10, 13 and 22, c) ref. 11 and the current work (below).

catalysis at high temperatures causes combustion and "coking" of ACs and justifies the use of more resistant carbon nanomaterials.[22] However, in a liquid-phase at low temperatures the degradation of AC is not an issue in oxidative carbocatalysis, which makes ACs highly appealing over the other allotropes (Scheme 1).

ACs are, in fact, commercially available in many forms and much cheaper than the other carbon (nano)materials. In addition, they are available as a high volume bulk product[23] and they can be prepared from non-fossil feedstock (e.g., lignin, cellulose, agricultural waste).[1,24] Furthermore, their catalytic activity can be enhanced by a simple, safe and ecological thermal treatment under air.[10] In contrast, the preparation of graphene oxide from graphite usually requires highly corrosive acids and strong oxidants, which are not only hazardous, but also generate significant amounts of toxic waste.[25] CNTs as well are usually treated, prior to their use in catalysis, by similarly strong oxidative conditions (i.e., refluxing nitric acid or $HNO_3:H_2SO_4$).[26] According to our rationale, AC-based carbocatalysis deserves further investigation in organic synthesis.

In the present study, we focused on oxidative dehydrogenative aromatization of saturated N-heterocycles, which is a convenient and atom-economic way to prepare unsaturated heterocycles. Previously, this route has been studied with homogeneous (Ir, Ru, Fe, Rh, Pd, Cu, Co) and heterogeneous (Ru, Cu, Au, Pd, Pt, Ni, Mn) transition metals on various supports.[27] Several metal-free approaches with graphene oxide (GO),[28] reduced graphene oxide (rGO),[29] mesoporous graphitic carbon nitride (mpg-C_3N_4),[30] polymaleimide,[31] and polydopamine have been published as well.[32] Interestingly, Hayashi and co-workers published several convincing reports where they used untreated ACs to synthesize anthracenes, pyridines, pyrazoles and indoles

under mild oxidative conditions.[11,33–36] Furthermore, they demonstrated that untreated AC delivers higher yields of quinolines and isoquinolines than Pd/C in MeCN.[37] In this work, we show that the catalytic activity of untreated AC in oxidative dehydrogenative aromatizations can be significantly improved by an operationally easy thermal treatment, and we apply this sustainable synthetic protocol for the synthesis of the indole core structure of progesterone receptor antagonists.
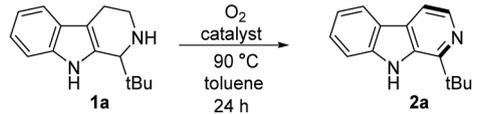
Results and discussion

We began our study by screening several carbon materials as catalysts for the ODH aromatization of 1-tert-butyl-1,2,3,4-tetrahydro-β-carboline (**1a**) to the corresponding β-carboline (**2a**) in toluene over 24 h at 90 °C under O_2-atmosphere (Table 1). The use of HCl washed commercial active carbon (AC_{dm}) delivered **2a** in 34% yield (entry 1). Surprisingly, yield increased only by 2% when HNO_3-oxidized active carbon (oAC_{HNO3}) was used as catalyst, as in previous studies we found this catalyst to be highly suitable for the homocoupling of heteroaryls (entry 2).[12] Similarly, 57% of **2a** was received when AC_{dm} was oxidized thermally under static air (oAC_{air}, entry 3). We then subjected this material to a thermal post-treatment under Ar at 425 °C, which is known to remove carboxylates selectively.[38] The obtained material ($oAC_{air(\Delta)}$) gave a slightly better yield of 59% (entry 4). The reaction conditions were optimized using a rather high, 896 mg $mmol^{-1}$, catalyst loading, equal to four weight equiv. of **1a**, which was the utmost limit that allowed efficient stirrability of the reaction suspension (0.25 M) using 24 h reaction time. Furthermore, widely used carbonaceous catalyst GO and its reduced form rGO delivered yields of 1% and 52%, respectively (entries 5 and 6). Previously, we have reported rather good results for ODH C–C couplings of aryls with HNO_3-oxidized carbon nanotubes (oCNT, entry 7),[15] but for the current reaction, this catalyst delivered only 20% yield.

Next, we performed reference tests to identify the possible active sites of the carbocatalyst. In absence of any catalyst, we received only 2% of **2a** (entry 8). We then employed different model compounds that have been used before to mimic the active sites in carbocatalysts.[39,40] Tetracene and anthraquinone delivered only marginal yields of 1% and 2% (entries 9–10). Remarkably, phenanthrenequinone produced 33% and 22% of **2a** under O_2 and Ar atmospheres, respectively (entry 11). All the results suggest that the quinoidic groups function as the active sites of the catalyst, which is in accordance with the characterization of the material (vide infra) and the literature.[2,20,36]

To expose the critical reaction parameters, the standard conditions were varied (Table 2). Decreasing the catalyst loading to one and two equivalents also decreased the yield to 30% and 42%, respectively (entries 2,3). Interestingly, increasing the reaction time to 72 h increased the yield to 67%, while decreasing it to 3 h resulted in 44% yield (entries

This journal is © The Royal Society of Chemistry 2021

Catal. Sci. Technol., 2021, **11**, 5962–5972 | **5963**

Table 1 Screening of carbocatalysts and model compounds

Entry	Catalyst[a]	Yield[b] (%)
1	AC_{dm}	34
2	oAC_{HNO3} (HNO_3 oxidized AC_{dm})	36
3	oAC_{air} (air oxidized AC_{dm} at 425 °C)	57
4	$oAC_{air(\Delta)}$ (air oxidized, decarboxylated[e])	59
5	GO^c	1
6	rGO	52
7	$oCNT^d$	20
Model compounds for carbon material:		
8	—	2
9	Tetracene (0.5 equiv.)	1
10	Anthraquinone (0.5 equiv.)	2
11	Phenanthrenequinone (0.5 equiv.)	33 (22)[f]

[a] Catalyst loading = 896 mg mmol^{-1} of SM (0.25 M). [b] As determined by ^1H NMR spectroscopy using 1,3,5-trimethoxybenzene as an internal standard. [c] 2.00 weight equiv., few layer modified Hummer's (cheaptubes.com). [d] Ref. 15. [e] By thermal treatment under Ar for 24 h at 450 °C (ESI[1]). [f] Under Ar (24 h).

Table 2 Variation of the reaction conditions in the aromatization of tetrahydro-β-carboline **1a** ODH
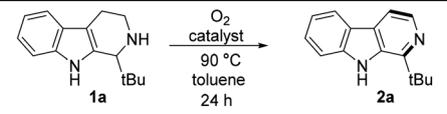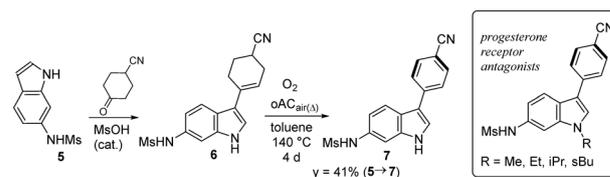
Entry	Variation from the standard conditions[a]	Yield (%)
1	—	59
2	25% catalyst loading (224 mg)	30
3	50% catalyst loading (448 mg)	42
4	Reaction time = 3 h	44
5	Reaction time = 72 h	67
6	T = RT	26
7	Anisole as solvent at 140 °C	67
8	Under Ar	24
9	1 equiv. MsOH additive	22
10	No catalyst	2

[a] 896 mg mmol^{-1} of SM (0.25 M).

4 and 5). Drastic differences were also observed upon changing the temperature. At room temperature, the reaction proceeded poorly with a low yield of 26% (entry 6), while in contrast we obtained **2a** in 67% yield when we raised the temperature to 140 °C (entry 7). We performed the latter experiment in anisole, which in addition to its higher boiling point, also has complementary value both in terms of safety and environmental profile.[41,42] Based on literature,[6–8,11] we supposed that molecular oxygen was acting as the terminal oxidant, so we investigated its role by running the reaction under inert atmosphere (Table 2, entry 8). Surprisingly, we obtained 24% yield, despite thorough removal of oxygen from the reaction mixture. This modest activity suggests a possible stoichiometric interaction occurring under Ar atmosphere with the presumed quinoidic active sites (*vide infra*). An addition of MsOH (entry 9), which was previously crucial for the carbocatalysed coupling of benzofused heterocycles,[12] decreased the yield

drastically to 22%. In the absence of carbocatalyst, only 2% yield was received (entry 10).

With the optimized conditions at hand, we studied the scope of ODH aromatization with 1,2,3,4-tetrahydro-β-carbolines, 1,2,3,4-tetrahydroquinolines and related tetrahydroaryl N-heterocyclic structures (Scheme 2). Due to the observed difference in reactivity between oAC_{HNO3} and $oAC_{air(\Delta)}$ during the synthesis of 1-*tert*-butyl-β-carboline (**2a**,

Scheme 2 One pot synthesis of progesterone receptor antagonist related 3-aryl indole **7**.

5964 | *Catal. Sci. Technol.*, 2021, **11**, 5962–5972

This journal is © The Royal Society of Chemistry 2021

Table 1), we screened the dehydrogenation of various tetrahydro N-heterocycles with both the catalysts. The complete list is presented in Table S1 (ESI†), but for most of the substrates $oAC_{air(\Delta)}$ was more active (Scheme 2).

We first explored the preparation of β-carboline substructures within the well-known harmala alkaloid family (Table 3, entries 1–5), using 6-methoxy-β-carboline as well.

We observed that upon addition of a methoxy substituent at C6 and removal of tBu from C1, the yield dropped from 59% (2a) to 38% (6-methoxy-β-carboline, 2b). The yield was lowered even more drastically for harmine 2c (12%) and isoharmine 2d (7%). Additionally, for the substrates 1a–1d the dihydro-imine intermediates could be isolated (see ESI†). On the other hand, 1-phenyl-substituted substrate 1x

Table 3 Dehydrogenation of tetrahydro N-heterocycles (isolated yields)

Entry	Substrate	Product(s)	Time (h)	Isolated yield (%)
1	1a	2a	24	59
			72	67
2	1x	2x	24	75
			72	86
3	1b	2b	24	38
4	1c	2c [3,4-dihydro-2c]	24	9^b $[15]^b$
5	1d	2d [3,4-dihydro-2d]	24	11 [9]
6	2e R = H; 2f R = OMe; 2g R = Me; 2h R = F; 2i R = Cl; 2j R = Br; 2k R = CO₂Me; 2l R = CN		24	≥99; 91^c; 92^c; 97^c; 72^c; 66^c; 96^c; 93^c
7	1m	2m	24	56^b
8	1n	2n	24	55^b
9	1o	2o	24	67
10	1p	2p [3,4-dihydro-2p]	24	30 [64]
11	1q	2q [3,4-dihydro-2q]	24	40 [9]
12	1r	2r	24	78

^{a} Catalyst loading: 896 mg mmol^{-1} of SM (0.25 M). ^{b} oAC_{HNO3} as catalyst. ^{c} ^{1}H NMR average yield of two runs (1,3,5-trimethoxybenzene as internal standard). [Dihydrointermediates in brackets].

This journal is © The Royal Society of Chemistry 2021

Catal. Sci. Technol., 2021, 11, 5962–5972 | 5965

exhibited higher reactivity, and was converted with 75% yield to **2x** in 24 h (86% yield in 72 h). We then moved to study various quinoline-derivatives. All 6-substituted 1,2,3,4-tetrahydroquinolines (THQs) were dehydrogenated in excellent to quantitative yields. Notable exceptions were 6-bromo and 6-chloro derivatives that were obtained in 66% and 72% yields, respectively (Table 3, entry 6). Quinoxaline (**2o**) was dehydrogenated from its 1,2,3,4-tetrahydro precursor in 67% yield and 1,2,3,4-tetrahydroisoquinoline (**1q**, THIQ) was converted to isoquinoline in 40% yield. The yield of isoquinoline could be further improved to 67% by extending the reaction time to 72 h and raising the temperature from 90 °C to 100 °C. Slightly better yields were received with oAC$_{HNO3}$ (56% and 55%) than with oAC$_{air(\Delta)}$ (53% and 47%) for quinaldine (**2m**) and 2,6-dihydroxyquinoline (**2n**), respectively.

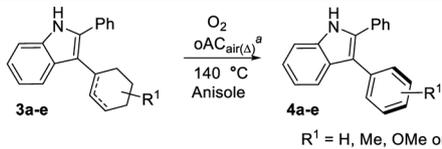To prove the catalytic nature of the carbon material, we performed an additional test with 1-phenyl-1,2,3,4-tetrahydro-β-carboline (**1x**) ODH to **2x**. At the first stage, the reaction was run for 24 h under argon at otherwise standard conditions (Table 2). Thereafter, at the second phase, the atmosphere was exchanged to O$_2$ and the reaction was stirred for an additional 24 h. After the first step, the reaction delivered only 35% yield, however, when the second stage was completed, 71% of **2x** was received. The test proves that the oxygen reactivates the consumed catalyst, reinitiating the catalytic cycle.

Next, we became curious whether we could extend the ODH method to the aromatization of 2-phenyl-3-(cyclohexenyl)-indoles to the corresponding 2,3-diphenylindole derivatives. Initially, when the optimized conditions for the previous ODH aromatizations were used,

we could only obtain products in low yields. However, when we changed the solvent to anisole and raised the temperature to 140 °C we obtained 1H-2,3-diphenylindole in 61% yield. The scope of the reaction was explored using 2-phenyl-indole as the backbone structure and varying the 3-tetrahydroaryl substituent (Table 4). Overall, the yields for most 3-aryl-2-phenyl-indoles were moderate, varying between 49–72% with 24–72 h reaction time. Interestingly, 3-(4-methoxy-tetrahydroaryl)-2-phenyl-indole (**3d**) yielded mainly the elimination product 2,3-diphenyl-indole (**4a**). Interestingly, a control test in the absence of carbocatalyst yielded only 4% of **3b** after 72 h reaction time.

As 3-tetrahydroaryl indoles can be straightforwardly prepared via a condensation reaction between indoles and the cyclohexanones (see ESI†), the developed methodology does not only open a concise synthetic route, but also a transition metal-free access to biaryl compounds that are typically prepared with Pd-mediated couplings (in this case by Suzuki–Miyaura couplings) from halide and boronic acid (or ester) functionalized aryls.[43] Importantly, the developed method allows the employment of unprotected (NH)-indoles as substrates that are often not tolerated in Pd-coupling reactions.[44] The development of this protocol is of significant synthetic relevance as many 3-aryl indoles are core structures of active pharmaceutical ingredients of marketed drugs.[44] In order to test the viability of the concept, we synthesized 3-aryl indole 7 that is the core structure of the progesterone receptor antagonists (Scheme 2).[45] The synthesis was carried out in only two steps with 41% yield without prefunctionalization or N-protection, while the reported Pd-coupling protocols required halogen functionalization at the indole C3 position

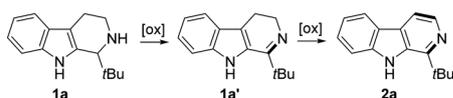**Table 4** Dehydrogenation of 3-(tetrahydroaryl)-2-phenyl-indoles

Entry	Substrate		Time (h)	Isolated yield (%)
1		**3a**	24	61
2		**3b**	72	49
3	Me	**3c**	72	52
4	OMe	**3d**	24	Traces[b]
5				(69% **4a** R^1 = H)
6	Me	**3e**	24	72
7	CF$_3$	**3f**	24	65
8		**3b**	72	4[c,d]

[a] 896 mg mmol^{-1} of SM (0.25 M). [b] Identified in HRMS. [c] Test run with no catalyst. [d] NMR yield.

5966 | *Catal. Sci. Technol.*, 2021, **11**, 5962–5972

This journal is © The Royal Society of Chemistry 2021

and 4–6 steps to deliver the product or other 3-aryl indole analogues.[45]

Kinetic monitoring of **1a** with ^1H NMR, performed with both oAC_{HNO3} and $oAC_{air(\Delta)}$, indicates that the dehydrogenation reaction to **2a** proceeds *via* 3,4-dihydro intermediate (Fig. 1a). The reaction monitoring also demonstrates the better catalytic activity of the air oxidized catalyst compared to the HNO_3 oxidized one (Fig. 1b). Based on our previous oAC studies,[12] and reference compound stoichiometric experiments (see phenanthrenequinone in Table 1), we presume that the quinoidic groups are the active sites in oAC catalysts. To support this hypothesis, we analysed the employed carbocatalysts with X-ray photoelectron spectroscopy (XPS) to evaluate their surface properties (see ESI†). From the survey spectra it was possible to determine the O% of each sample, and evaluate the efficacy of each catalyst preparation protocol in introducing O-containing groups (Tables S2 and S3†). When compared to AC_{dm} (Fig. 2a), oAC_{HNO3} exhibits a higher amount of $C=O$
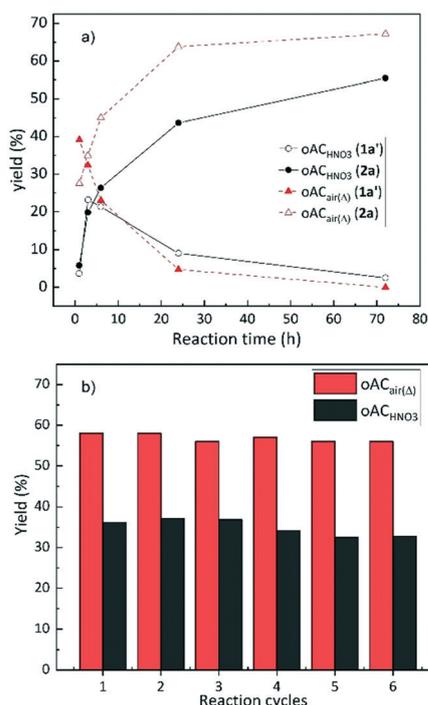

Fig. 1 a) Kinetic ^1H NMR monitoring of **1a** conversion to **2a** *via* **1a'** (3,4-dihydrocarbazole) intermediate catalysed by $oAC_{air(\Delta)}$ (red curve) and oAC_{HNO3} (black curve) at 90 °C (working up the reaction at each time point), b) catalysts recyclability test over 6 cycles in toluene with oAC_{HNO3} (black bars) and $oAC_{air(\Delta)}$ (red bars) for 24 h under O_2 at 90 °C. After each run, the catalyst was filtered off and washed thoroughly with CH_2Cl_2/MeOH (93/7). The yield was determined by ^1H-NMR using 1,3,5-trimethoxybenzene as an internal standard.

groups, as well as abundant C–OH and $O–C=O$ groups, while the oxidation occurs with concurrent deterioration of the graphitic surface $C(sp^2, \pi–\pi^*)$. In contrast, the thermal air-oxidation (oAC_{air}) is gentler on the π-surface, but also produces less oxygen containing functional groups. Raman measurements (ESI†) support this assumption, as higher I_D/I_G ratio was calculated for oAC_{HNO3} (1.02) than for $oAC_{air(\Delta)}$ (0.97), indicating increased defectivity and reduction of graphene-type domains in the HNO_3-oxidized carbon.

The thermal decarboxylative post-treatment under Ar notably increases the relative $C=O$ content in the $oAC_{air(\Delta)}$ material. Based on combined material characterization, the nitric acid treatment is more efficient in promoting the formation of oxygen functionalities. However, the O1s peak deconvolution (Table 5) reveals that there is a significant difference in acidic group abundance between oAC_{HNO3} and $oAC_{air(\Delta)}$, which seems to be critical for the catalytic activity towards the explored reactions. Similar poor reactivity was also demonstrated for GO (Table 1), where the high degree of oxidation and abundance of –COOH groups are both characteristic features.[46] The oxygen containing functional group content was also examined with temperature-programmed desorption (TPD). The CO_2 desorption curve (Fig. 2c) highlights the divergent abundance of carboxylic acid groups in the two different materials; absence in $oAC_{air(\Delta)}$ and high distribution in oAC_{HNO3}, confirming the XPS results. From the CO desorption curves (Fig. 2d), it is noticeable how both materials are rich in carbonyls, although $oAC_{air(\Delta)}$ displays an additional shoulder at higher temperature (>800 °C) that can be associated with quinones and basic functionalities such as chromenes and pyrones (deconvolution of the TPD curves are presented in ESI†). This feature was confirmed by MAS NMR (Fig. 2b): the broad peak appearing around 190–200 ppm in $oAC_{air(\Delta)}$ spectrum is further evidence of higher abundance of quinones.

Textural properties were analyzed with N_2 physisorption (Fig. S26†). Both catalysts present adsorption isotherms of the type I plus II that implies the presence of micro- and mesopores within the materials. The hysteresis loops of type H4 are associated with a narrow slit-like mesopores. The BET surface area appears to slightly decrease with the nitric acid treatment, while it increases in the case of air oxidation (Table S8†). The increased available surface can be recognized as another feature contributing to the better catalytic performance of $oAC_{air(\Delta)}$.

Next, we analyzed the combined effect of high surface area and carbonyl content on the catalyst activity for the dehydrogenation of both 1-*tert*-butyl-1,2,3,4-tetrahydro-β-carboline (**1a**) and 1,2,3,4-tetrahydroquinoline (**1e**) (Fig. 3). For both reactions, a direct correlation between these parameters can be noticed: the highest yields are obtained when there is a combination of high surface area and high carbonyl content. One exception to this trend is oAC_{HNO3}, which stands out due to its lower catalytic activity, despite having the highest $C=O$% and high surface area. The moderate obtained yields can be ascribed to its high
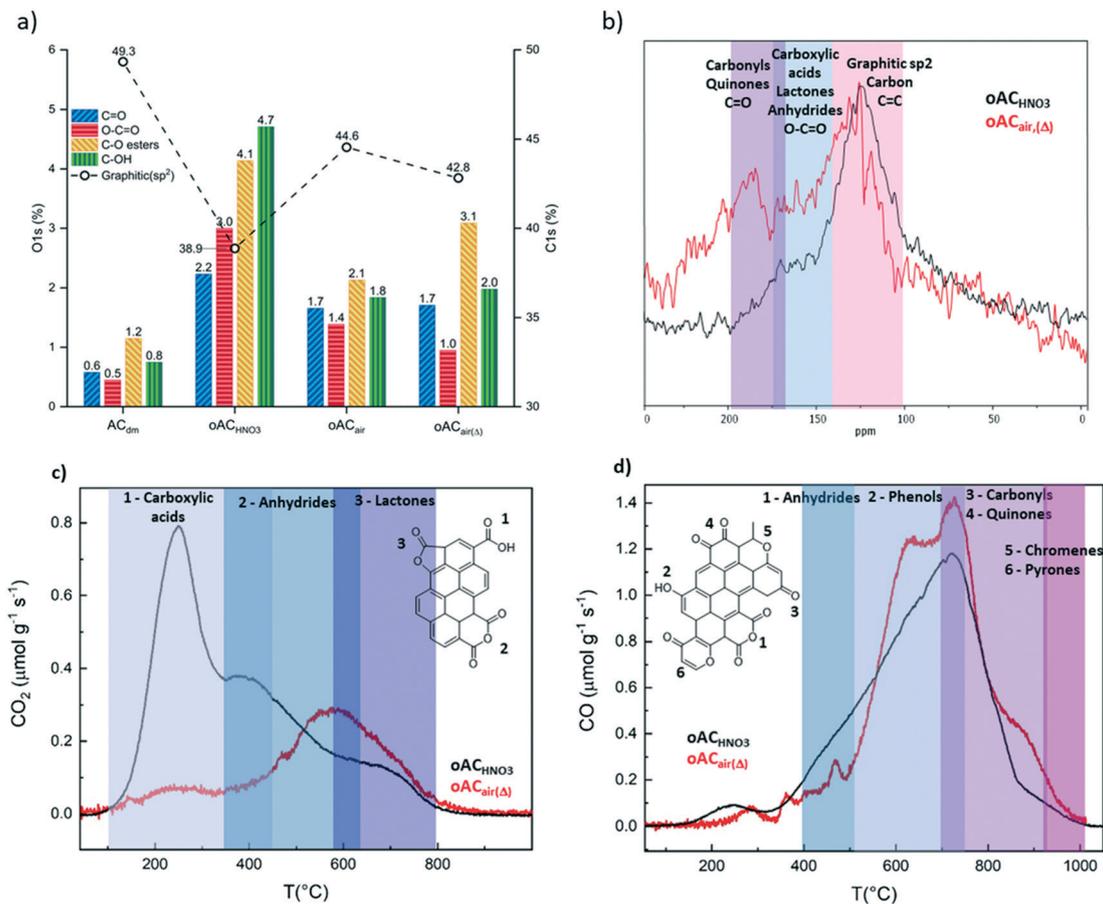
Fig. 2 a) Atomic percentages from XPS O1s (bars) and C1s (graphic, sp²) (dashed line with circles) spectra. AC_{dm}, oAC_{HNO3}, oAC_{air}, and $oAC_{air(\Delta)}$, represent HCl-washed, HNO_3 oxidized, air oxidized, and thermally treated air oxidized active carbons, respectively, b) MAS NMR spectra of oAC_{HNO3} (black) and $oAC_{air(\Delta)}$ (red), c) CO_2 and d) CO TPD profiles of desorption from the surface of oAC_{HNO3} (black) and $oAC_{air(\Delta)}$ (red) during heating in an inert atmosphere, with marked regions of desorption temperatures and corresponding structures of oxygen functionalities.

Table 5 Summary of O1s XPS peak deconvolutions for $oAC_{air(\Delta)}$ a) before and b) after, and oAC_{HNO3} c) before and d) after the recycling (the values are in %)
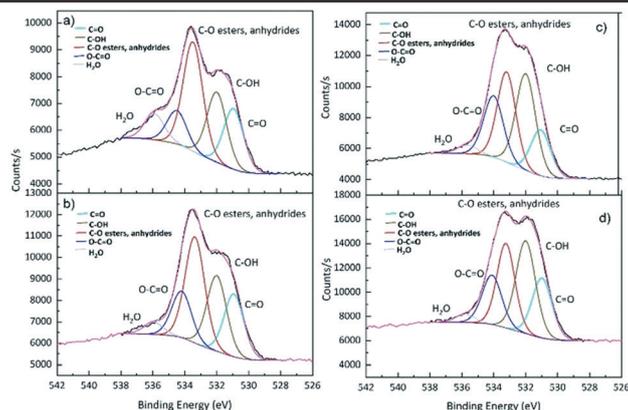
Material	H_2O	O–C=O	C–O esters, anhydrides	C–OH	C=O	N (pyrrolic)
Peak BE (eV)	535.9	524.2	533.3	532.3	531.1	400.33
oAC_{HNO3}	0.39	2.29	4.79	4.51	2.21	
oAC_{HNO3} recycled	0.34	2.09	3.27	3.91	2.53	3.19
$oAC_{air(\Delta)}$	0.73	0.93	3.04	1.95	1.69	
$oAC_{air(\Delta)}$ recycled	0.35	1.37	3.12	2.23	1.85	1.78

5968 | *Catal. Sci. Technol.*, 2021, **11**, 5962–5972

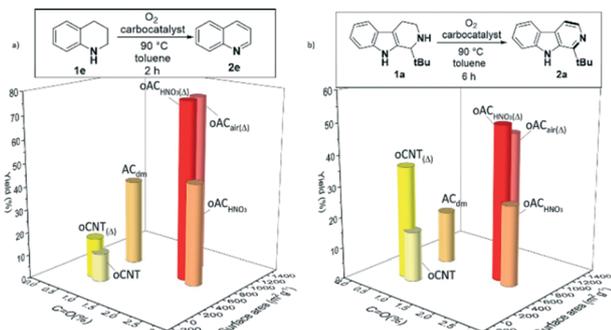This journal is © The Royal Society of Chemistry 2021

Fig. 3 Percent yield of dehydrogenation *versus* carbon surface area *versus* C═O% content (XPS) for a) 1-*tert*-butyl-1,2,3,4-tetrahydro-β-carboline and b) 1,2,3,4-tetrahydroquinoline, under aerobic conditions, after 2 h and 6 h reaction time, respectively (surface area of oCNT(Δ) was not measured).

carboxylic acid content, which appears to inhibit the studied reactions. To gain further proof of this, oCNTs and oAC_{HNO3} were subjected to the same decarboxylation treatment as $oAC_{air(\Delta)}$ (450 °C for 24 h under Ar atmosphere), which caused only minor changes in the materials' carbonyl content and surface area (see Fig. 3 and ESI†). These decarboxylated materials delivered remarkably increased yields for both reactions, proving that the high acid content has a detrimental effect for the studied ODH carbocatalysis.

Finally, the recyclability of the catalysts was tested to determine their robustness, as well as their catalytic nature. For this purpose, both oAC_{HNO3} and $oAC_{air(\Delta)}$ were used for six sequential cycles of 1-*tert*-butyl-1,2,3,4-tetrahydro-β-carboline (**1a**) dehydrogenation. Between the cycles, the carbocatalysts were filtered off and thoroughly washed with CH_2Cl_2/MeOH (93/7%). As shown in Fig. 1b, no major decrease in catalytic activity was observed, indicating robustness of both carbocatalysts. Therefore, we can state that the carbon materials act mainly as catalysts, only marginally taking part in the reaction in a stoichiometric way. This contrasts the recent report that casts some doubts over the catalytic nature of GO in (alcohol) oxidation reactions.[47] To further enforce our statement, the two carbocatalysts were analysed by XPS after the recycling experiments and the oxygen peaks were compared to the ones measured before the catalysis (Table 5). As summarized in Table 5, the changes in the oxygen groups' distribution are almost negligible in the both cases. Noticeably, a peak associated to pyrrolic Ns appears after the recycling, which can indicate a possible partial stoichiometric reactivity between the carbon and the substrate.

Inductively coupled plasma mass spectrometry (ICP-MS) was used to investigate the possible presence of residual metal impurities. The study revealed that the carbon materials examined contain a maximum of 600 ppm level of Fe and notably lower amounts of other metal impurities (*e.g.*, in $oAC_{air(\Delta)}$: Ni < 30 ppm, Mn = 40 ppm, Cu = 20 ppm, Co < 3 ppm and Pd < 0.2 ppm; Table S4†), which makes trace metal impurity catalysis unlikely. The high carbon material

loadings used in the catalytic runs may raise questions about the actual catalytic nature of oACs. TPD analysis of $oAC_{air(\Delta)}$ shows that the total concentration of carbonyls and quinones is 1861 μmol g^{-1}, which makes the loading for each catalytic cycle appear quite high (416 μmol for 250 μmol of starting material). Anyhow, this theoretical maximum of catalytically active quinone sites is calculated presuming that all the carbonyls are in quinone-type configurations and that they are accessible by the substrates, which is questionable, as ACs have high microporous surface areas (see BET analysis Fig. S32†). The model compound studies strongly suggests that only some quinone configurations are active in the catalytic process. Considering that TPD analysis does not discriminate the different configurations of quinones and carbonyls, we can assume that the actual number of redox active sites for each run is considerably lower. This consideration, together with the good recyclability of the carbocatalyst shines a light on the reason why such high catalyst loading is required, mitigating the doubts on the actual catalytic nature of the material.

We then turned our attention to the reaction mechanism of the oxidative carbocatalyzed aromatizations. We chose THQs as mechanistic probes as they were the most reactive substrates, and different 6-R-THQs (see Scheme 2) can be easily prepared or are commercially available.

Quinoidic groups have been pinpointed by various studies as the mediators of carbon catalysed dehydrogenations in both gas[14] and liquid phase.[36] Furthermore, they have been also identified as active sites in ODH C–C couplings of various (hetero)aryl substrates.[13,48,49] Usually, hydrogen abstraction is proposed as a reasonable mechanistic route in the gas-phase dehydrogenative reactions.[49] However, in liquid phase other mechanistic pathways become possible and the dehydrogenation does not necessarily need to proceed *via* neutral radical intermediates. The commonly proposed reaction mechanisms in homogeneous quinone-promoted oxidations include sequential electron–proton transfer, hydrogen atom transfer, and hydride transfer.[50] In addition, Stahl and coworkers have reasoned that the oxidation of THIQ with phenanthroline could take place *via* a hemiaminal pathway.[51,52] Building on these mechanistic proposals for both heterogeneous and homogeneous quinones, we consider the following alternatives: i) H-abstraction, ii) bimolecular hydride transfer, and iii) hemiaminal pathway.

Firstly, we performed the reaction in the presence of 1 equiv. of radical scavenger 2,2,6,6-tetramethylpiperidin-1-oxyl (TEMPO). Interestingly, TEMPO did not trap any radicals and neither had any influence on the received yields.

We then performed a Hammett plot study by varying the substituent at THQ's 6-position (Fig. 4). The observed negative ρ-value (−0.45 or −0.43, see Fig. 3a) suggested the formation of a positive charge in the transition state of the rate-limiting step.[53] Linear fitting without the halogen substituted substrates shows excellent correlation in Fig. 4a (R^2 = 0.999) between the σ_{para} values and $\log(k_X/k_H)$. The

This journal is © The Royal Society of Chemistry 2021

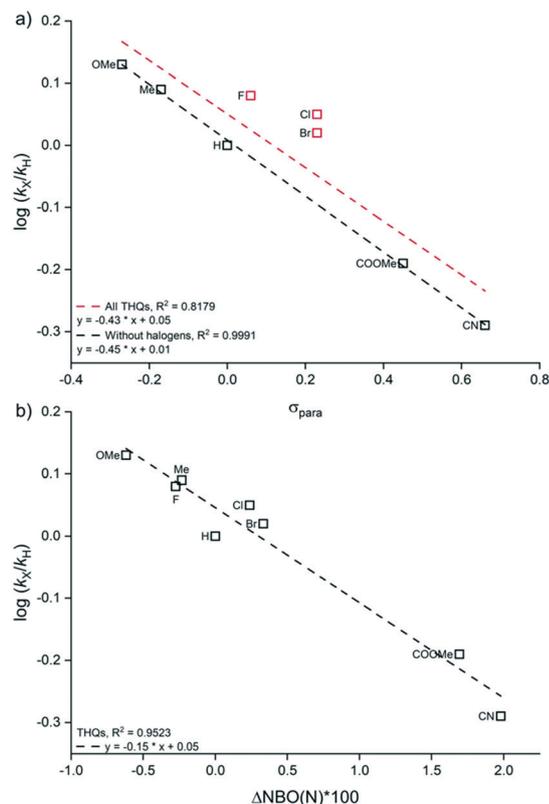*Catal. Sci. Technol.*, 2021, **11**, 5962–5972 | **5969**

Fig. 4 Hammett plot for 6-R-THQs: a) $\log(k_X/k_H)$ *versus* σ_{para} values, and b) $\log(k_X/k_H)$ *versus* ΔNBO(N) charges (see ESI†).

Scheme 3 Kinetic isotopic effect measurements for **1e** to **2e** conversions.

divergent results with the halogenated THQs can arise from the resonance effects not captured by the Hammett σ_{para} values.

After this, we considered direct bimolecular hydride transfer and the hemiaminal pathway, see Fig. 5 and S1 and S2,† which have been suggested for homogeneous quinones. To distinguish between the two different mechanisms, and to identify whether the first hydride abstraction takes place from the 2- or 4-position (Scheme 3), we synthesized deuterated analogues of **1e** and measured the kinetic isotope
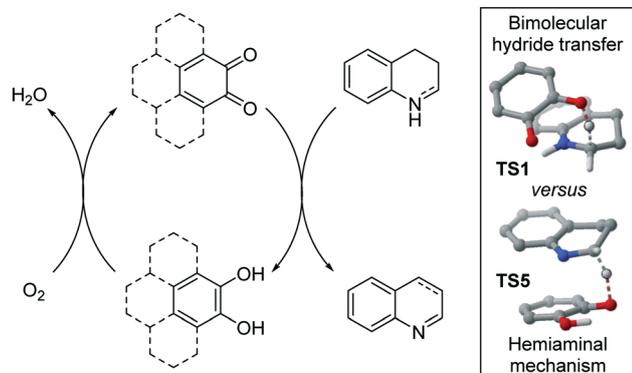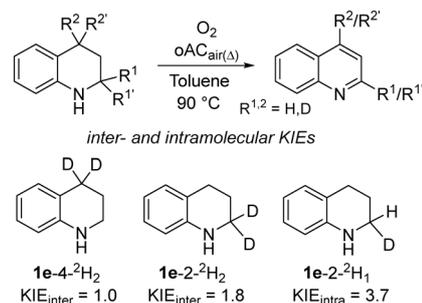
effects. Comparing the intermolecular KIEs between **1e**, **1e**-2-^{2}H$_2$, and **1e**-4-^{2}H$_2$ revealed that there is no observable ^{1}H/^{2}H KIE on C4, whereas C2 exhibited KIE of 1.8. Therefore, the rate-determining H-abstraction occurs from the C2-position. Additionally, the observed KIE rules out a rate-determining electron transfer followed by fast deprotonation.[54,55] However, the intramolecular KIE with **1e**-2-^{2}H$_1$ was higher than the intermolecular KIE; 3.7 *versus* 1.8, respectively (Scheme 3). Stahl and coworkers have earlier argued that the divergent intra−/intermolecular KIE values support the formation of a pre-equilibrium transient covalent adduct prior to the hydride transfer.[55] However, it has also been debated that the said pre-equilibrium adduct is an off-cycle species[56] or even contradicts high intermolecular KIE values in related reduction reactions of dihydropyrans with PhC(O)CF$_3$.[57]

We then decided to compute the activation free energies for the dehydrogenation reaction for both hydride transfer and hemiaminal pathway mechanisms. We selected phenanthrenequinone (PQ) and *ortho*-benzoquinone (*o*-BQ) as the model quinoidic fragments[15] and **1e** as the model substrate. The computed activation free energy barriers indicate that the rate-determining steps for both mechanisms – hydride transfer (**TS1**) and hemiaminal pathway (**TS5**) – are energetically close (see Fig. 5 and ESI†): $\Delta G^{\ddagger}(\textbf{TS1}_{o\text{-BQ}}) = 27.1$ kcal mol^{-1} *versus* $\Delta G^{\ddagger}(\textbf{TS5}_{o\text{-BQ}}) = 28.5$ kcal mol^{-1} and $\Delta G^{\ddagger}(\textbf{TS1}_{PQ}) = 31.3$ kcal mol^{-1} *versus* $\Delta G^{\ddagger}(\textbf{TS5}_{PQ}) = 35.4$ kcal mol^{-1}. Therefore, the mechanisms can coexist, see ESI† for details. The activation free energy barriers are, however, dependent on the properties of the model quinone, *i.e.*, reduction potential, electrophilicity and hydride affinity, and thus accurate prediction of the activation free energies is not possible without accurate models of the carbon material.

Therefore, we compared the THQs' and hemiaminals' partial charges with the experimental reaction rates in Fig. 4b and S3 (ESI†). The NBO charge on THQs' nitrogen correlated well ($R^2 = 0.9523$) with the measured reaction rates, including the halogenated substrates, while the hemiaminals' nitrogen NBO charges gave poor correlations with the experimental reaction rates with R^2-values less than 0.8610 (see ESI†). Thus, the experimental and computational studies indicate that the bimolecular hydride transfer is the operative mechanism with the THQs and the employed carbocatalyst,

Fig. 5 Proposed mechanism for THQ dehydrogenation. Plausible overall catalytic cycle (left) and the transition states (**TS1** and **TS5**) for the two proposed mechanisms (right).

5970 | *Catal. Sci. Technol.*, 2021, **11**, 5962–5972

This journal is © The Royal Society of Chemistry 2021

although both mechanisms are viable. Currently, profound studies are ongoing in our laboratory to elucidate the mechanism in more detail for all substrates.

Experimental

Preparation of Carbocatalysts

Preparation of AC$_{dm}$ (removal of metal impurities). 16.0 g of AC (1 kg batch (lot. H2430) from Fluka with 100 mesh particle size) were placed in a flask and 130 mL of 1 M HCl (aq.) were added. After stirring for 6 h at 70 °C, AC was filtered off and washed with 3 L of dist. H$_2$O. AC$_{dm}$ was dried in an oven at 140 °C for 16 h and was obtained in a yield of 16.0 g.

Preparation of oAC$_{HNO3}$. AC$_{dm}$ (4.00 g) was placed in a flask and 8 mL of nitric acid (68% aq.) was slowly added forming a slurry. The flask was attached to a Dreschel bottle with NaOH aq., and then the flask was heated to 140 °C for 15 h. oAC was then dried in vacuum at 140 °C for 2 h, resulting in a yield of oAC$_{HNO3}$ of 3.88 g.

Preparation of oAC$_{air}$. AC$_{dm}$ (4.00 g) was placed in a porcelain crucible which was heated to 425 °C for 16 h (30 °C min^{-1}) in an oven in presence of air. oAC$_{air}$ was obtained in a yield of 3.11 g.

Preparation of oAC$_{air(\Delta)}$. oAC$_{air}$ (3.11 g) was placed in a tubular oven under Ar flow (40 cm^3 min^{-1}) for 23 h. The temperature was increased from RT to 450 °C (10 °C min^{-1}) and kept at 450 °C for 24 h while maintaining the Ar flow. After cooling to RT, oAC$_{air(\Delta)}$ was obtained in a yield of 3.05 g.

General procedure for Carbocatalytic oxidative dehydrogenations

Carbocatalyst and starting material were placed in a vial and the appropriate solvent was added. The vial was sealed with a cap with septum. The vial was evacuated and filled with the appropriate gas in 3 cycles and the reaction was stirred at an appropriate temperature. The carbocatalyst was then removed by filtration of the reaction mixture over a column of Celite, and was followed by washed with DCM/MeOH to obtain the products.

Conclusions

We have developed oxidized active carbon-based catalysts for the dehydrogenation of aryl fused N-heterocycles and 3-(cyclohexenyl)-indoles. The metal-free carbon materials operate in a catalytic fashion using O$_2$ as the terminal oxidant. With respect to N-heterocycle dehydrogenation, the developed oAC material offers improved efficiency compared to reported ACs and other reported carbon allotropes like GO and CNTs. Regarding 3-(cyclohexenyl)-indoles, we were able to demonstrate an alternative route for (hetero)biaryls that were previously obtained with multistep transition metal-mediated sequence. This opens a novel path for the synthesis of a family of indole-based medical compounds, traditionally relying on highly toxic chemicals as well as transition metal catalysis. The catalytic behaviour and robustness of the oACs was confirmed by recyclability tests, which showed remarkable stability over six cycles. While carbocatalyst development studies typically focus on determining the active sites and increasing their abundance, here we demonstrated that the catalyst performance is significantly improved by removing the inhibiting carboxyl groups from the carbon material. We expect that this work will pave the way for further development of carbon-based catalysts for ODH reactions to offer robust alternatives for transition metal mediated reactions.

Author contributions

L. E.: synthetic work, method development, writing – original draft; D. C.: method and catalyst development, catalyst testing; S. A.: theoretical (DFT) calculations, writing; A. L.: experimental work, analysis of results, writing – editing; T. W.: catalyst development, writing – editing, T. H.: XPS characterization; S. H.: solid state NMR; L.R. and M.F.P.: BET and TPD analysis; J. H.: supervision, writing – editing, project administration.

Conflicts of interest

There are no conflicts to declare.

Acknowledgements

References

1 *Activated Carbon*, ed. H. Marsh and F. Rodríguez-Reinoso, Elsevier, 1st edn, 2006.

2 J. L. Figueiredo and M. F. R. Pereira, *Carbon Materials for Catalysis. Carbon as Catalyst*, ed. P. Serp and J. L. Figueiredo, Wiley, 2008.

3 D. R. Dreyer and C. W. Bielawski, *Chem. Sci.*, 2011, **2**, 1233.

4 L. Liu, Y.-P. Zhu, M. Su and Z.-Y. Yuan, *ChemCatChem*, 2015, **7**, 2765–2787.

5 D. S. Su, G. Wen, S. Wu, F. Peng and R. Schlögl, *Angew. Chem., Int. Ed.*, 2017, **56**, 936–964.

6 D. R. Dreyer, H.-P. Jia and C. W. Bielawski, *Angew. Chem., Int. Ed.*, 2010, **49**, 6813–6816.

7 S. Mao, B. Li and D. S. Su, *J. Mater. Chem. A*, 2014, **2**, 5287–5294.

8 R. S. Drago and K. Jurczyk, *Appl. Catal., A*, 1994, **112**, 117–124.

9 M. F. R. Pereira, J. J. M. Órfão and J. L. Figueiredo, *Carbon*, 2002, **40**, 2393–2401.

10 M. F. R. Pereira, J. J. M. Órfão and J. L. Figueiredo, *Appl. Catal., A*, 1999, **184**, 153–160.

This journal is © The Royal Society of Chemistry 2021

Catal. Sci. Technol., 2021, **11**, 5962–5972 | 5971

11 M. Hayashi, *Chem. Rec.*, 2008, **8**, 252–267.

12 (*a*) T. Wirtanen, M. K. Mäkelä, J. Sarfraz, P. Ihalainen, S. Hietala, M. Melchionna and J. Helaja, *Adv. Synth. Catal.*, 2015, **357**, 3718–3726; (*b*) D. S. Casadio, S. Aikonen, A. Lenarda, M. Nieger, T. Hu, S. Taubert, D. Sundholm, M. Muuronen, T. Wirtanen and J. Helaja, *Chem. – Eur. J.*, 2021, **27**, 5283–5291; (*c*) M. K. Mäkelä, E. Bulatov, K. Malinen, J. Talvitie, M. Nieger, M. Melchionna, A. Lenarda, T. Hu, T. Wirtanen and J. Helaja, Carbocatalytic Cascade Synthesis of Polysubstituted Quinolines from Aldehydes and 2-Vinyl Anilines, *Adv. Synth. Catal.*, 2021, DOI: doi.org/10.1002/adsc.202100711.

13 J. Zhang, D. Su, A. Zhang, D. Wang, R. Schlögl and C. Hébert, *Angew. Chem., Int. Ed.*, 2007, **46**, 7319–7323.

14 M. Melchionna, S. Marchesan, M. Prato and P. Fornasiero, *Catal. Sci. Technol.*, 2015, **5**, 3859–3875.

15 T. Wirtanen, S. Aikonen, M. Muuronen, M. Melchionna, M. Kemell, F. Davodi, T. Kallio, T. Hu and J. Helaja, *Chem. – Eur. J.*, 2019, **25**, 12288–12293.

16 D. R. Dreyer, H.-P. Jia and C. W. Bielawski, *Angew. Chem., Int. Ed.*, 2010, **49**, 6813–6816.

17 J. Vijaya Sundar and V. Subramanian, *Org. Lett.*, 2013, **15**, 5920–5923.

18 H.-P. Jia, D. R. Dreyer and C. W. Bielawski, *Adv. Synth. Catal.*, 2011, **353**, 528–532.

19 *From metal to Metal-Free Catalysts: Routes to Sustainable Chemistry*, ed. M. Monai, M. Melchionna and P. Fornasiero, Academic Press, 2018, ch. 1, pp. 1–73.

20 M. S. Ahmad and Y. Nishina, *Nanoscale*, 2020, **12**, 12210–12227.

21 W. Qi and D. Su, *ACS Catal.*, 2014, **4**, 3212–3218.

22 J. Zhang, X. Liu, R. Blume, A. Zhang, R. Schlögl and D. S. Su, *Science*, 2008, **322**, 73–77.

23 In year 2015, global market of activated carbon was 2,743.4 KT with 8.1 billion USD market value. The market is projected to grow in next years. https://www.marketsandmarkets.com.

24 K. Ukanwa, K. Patchigolla, R. Sakrabani, E. Anthony and S. Mandavgane, *Sustainability*, 2019, **11**, 6204.

25 P. P. Brisebois and M. Siaj, *J. Mater. Chem. C*, 2020, **8**, 1517–1547.

26 K. A. Wepasnick, B. A. Smith, K. E. Schrote, H. K. Wilson, S. R. Diegelmann and D. H. Fairbrother, *Carbon*, 2011, **49**, 24–36.

27 W. Zhou, Q. Tao, F. Sun, X. Cao, X. Qian, J. Xu, M. He, Q. Chen and J. Xiao, *J. Catal.*, 2018, **361**, 1–11.

28 J. Zhang, S. Chen, F. Chen, W. Xu, G.-J. Deng and H. Gong, *Adv. Synth. Catal.*, 2017, **359**, 2358–2363.

29 N. Morimoto, Y. Takeuchi and Y. Nishina, *Chem. Lett.*, 2016, **45**, 21–23.

30 F. Su, S. C. Mathew, L. Möhlmann, M. Antonietti, X. Wang and S. Blechert, *Angew. Chem., Int. Ed.*, 2011, **50**, 657–660.

31 Y. Zhang, S. Pang, Z. Wei, H. Jiao, X. Dai, H. Wang and F. Shi, *Nat. Commun.*, 2018, **9**, 1465.

32 S. A. Pawar, A. N. Chand and A. V. Kumar, *ACS Sustainable Chem. Eng.*, 2019, **7**, 8274–8286.

33 Y. Kawashita, N. Nakamichi, H. Kawabata and M. Hayashi, *Org. Lett.*, 2003, **5**, 3713–3715.

34 N. Nakamichi, H. Kawabata and M. Hayashi, *J. Org. Chem.*, 2003, **68**, 8272–8273.

35 M. Hayashi, Y. Nomura and Y. Kawashita, *Heterocycles*, 2007, **74**, 629.

36 Y. Kawashita, J. Yanagi, T. Fujii and M. Hayashi, *Bull. Chem. Soc. Jpn.*, 2009, **82**, 482–488.

37 T. Tanaka, K. Okunaga and M. Hayashi, *Tetrahedron Lett.*, 2010, **51**, 4633–4635.

38 J. L. Figueiredo, M. F. R. Pereira, M. M. A. Freitas and J. M. Órfão, *Carbon*, 1999, **37**, 1379–1389.

39 S. Wu, G. Wen, X. Liu, B. Zhong and D. S. Su, *ChemCatChem*, 2014, **6**, 1558–1561.

40 H. Wu, C. Su, R. Tandiana, C. Liu, C. Qiu, Y. Bao, J. Wu, Y. Xu, J. Lu, D. Fan and K. P. Loh, *Angew. Chem., Int. Ed.*, 2018, **57**, 10848–10853.

41 D. Prat, A. Wells, J. Hayler, H. Sneddon, C. R. McElroy, S. Abou-Shehada and P. J. Dunn, *Green Chem.*, 2016, **18**, 288–296.

42 C. M. Alder, J. D. Hayler, R. K. Henderson, A. M. Redman, L. Shukla, L. E. Shuster and H. F. Sneddon, *Green Chem.*, 2016, **18**, 3879–3890.

43 A. J. J. Lennox and G. C. Lloyd-Jones, *Chem. Soc. Rev.*, 2014, **43**, 412–443.

44 Y. Mohr, M. Renom-Carrasco, C. Demarcy, E. A. Quadrelli, C. Camp, F. M. Wisser, E. Clot, C. Thieuleux and J. Canivet, *ACS Catal.*, 2020, **10**, 2713–2719.

45 T. I. Richardson, C. A. Clarke, K.-L. Yu, Y. K. Yee, T. J. Bleisch, J. E. Lopez, S. A. Jones, N. E. Hughes, B. S. Muehl, C. W. Lugar, T. L. Moore, P. K. Shetler, R. W. Zink, J. J. Osborne, C. Montrose-Rafizadeh, N. Patel, A. G. Geiser, R. J. S. Galvin and J. A. Dodge, *ACS Med. Chem. Lett.*, 2011, **2**, 148–153.

46 D. R. Dreyer, S. Park, C. W. Bielawski and R. S. Ruoff, *Chem. Soc. Rev.*, 2010, **39**, 228–240.

47 S. Presolski and M. Pumera, *Angew. Chem., Int. Ed.*, 2018, **57**, 16713–16715.

48 H. Wu, C. Qiu, Z. Zhang, B. Zhang, S. Zhang, Y. Xu, H. Zhou, C. Su and K. P. Loh, *Adv. Synth. Catal.*, 2020, **362**, 789–794.

49 W. Qi, P. Yan and D. S. Su, *Acc. Chem. Res.*, 2018, **51**, 640–648.

50 C. A. Morales-Rivera, P. E. Floreancig and P. Liu, *J. Am. Chem. Soc.*, 2017, **139**, 17935–17944.

51 B. Li, A. E. Wendlandt and S. S. Stahl, *Org. Lett.*, 2019, **21**, 1176–1181.

52 A. E. Wendlandt and S. S. Stahl, *J. Am. Chem. Soc.*, 2014, **136**, 506–512.

53 C. Hansch, A. Leo and R. W. Taft, *Chem. Rev.*, 1991, **91**, 165–195.

54 B. W. Carlson and L. L. Miller, *J. Am. Chem. Soc.*, 1983, **105**, 7453–7454.

55 B. W. Carlson and L. L. Miller, *J. Am. Chem. Soc.*, 1985, **107**, 479–485.

56 D. M. Chipman, R. Yaniv and P. van Eikeren, *J. Am. Chem. Soc.*, 1980, **102**, 3244–3246.

57 C. L. Perrin and C. Zhao, *Org. Biomol. Chem.*, 2008, **6**, 3349–3353.

5972 | *Catal. Sci. Technol.*, 2021, **11**, 5962–5972

This journal is © The Royal Society of Chemistry 2021